IEEE Access
Multidisciplinary | Rapid Review | Open Access Journal

Received September 29, 2018, accepted October 26, 2018, date of publication October 30, 2018,
date of current version November 30, 2018.

*Digital Object Identifier 10.1109/ACCESS.2018.2878760*

# Compact Wideband Dual-Polarized Antenna With High Isolation Using Modified Direct Feeding Structure For Indoor Beamforming Array Applications

**YAOHUI ZHANG[1], DAOTONG LI[2], (Member, IEEE), YONGHONG ZHANG[1], AND YONG FAN[1], (Member, IEEE)**

[1]EHF Key Laboratory of Science, University of Electronic Science and Technology of China, Chengdu 611731, China
[2]Center of Aerocraft TT&C and Communication, Chongqing University, Chongqing 400044, China

Corresponding author: Daotong Li (dli@cqu.edu.cn)

This work was supported in part by the National Natural Science Foundation of China under Grant 61801059, in part by the Venture and Innovation Support Program for Chongqing Overseas Returnees under Grant cx2017095, in part by the Fundamental Research Funds for the Central Universities under Grant 106112017CDJXY500002, and in part by the Chongqing Special Found of Technology R&D for Academician under Grant cstc2018zdcy-yszxX0001.

**ABSTRACT** A modified direct feeding structure is proposed in this paper to realize a compact ($45 \times 45$ mm$^2$) wideband dual-polarized antenna with high isolation (33 dB) and low cross-polarization (30 dB). Compared with the conventional crossed dipole antennas, two additional pairs of dipoles are employed as coupling baluns as well as radiators. As a consequence, the proposed antenna with more symmetrical structure has the advantages of both the direct feeding (DF) and the coupling feeding (CF) structures, such as, balanced matching, high isolation, low cross-polarization, and compact size. Besides, the gap structure between adjacent dipoles is designed in elliptical shape to further improve the impedance matching. The proposed antenna realizes a wide impedance bandwidth over 51% (1.7–2.85 GHz) for VSWR $<1.5$. It is worth mentioning that the compact size and high isolation could greatly reduce the element spacing of beamforming antenna array. In order to investigate the performance of beamforming array, a two-element array fed by the out-of-phase power divider network is developed. The lowest operating frequency can be further extended to 1.6 GHz and the cross-polarization discrimination (XPD) is more than 10 dB within $\pm 60°$ of the main lobe.

**INDEX TERMS** Modified direct feeding structure, compact, high isolation, wideband, dual-polarized.

## I. INTRODUCTION

In order to meet the demand of 2G/3G/4G communication systems, various kinds of broadband dual-polarized antennas, covering 1.71-2.69 GHz, have been developed for wireless communication base stations to alleviate the multipath fading and increase the channel capacity. In the outdoor base station applications, stable HPBW of $65° \pm 5°$ at the horizontal plane is required. Moreover, in the indoor base station applications, in order to achieve the specified radiation pattern, smaller element spacing is desired to place more antenna elements on a fixed-size metallic ground. Therefore, designing dual-polarized wideband antennas with compact size and high isolation is becoming a challenge for antenna researchers.

Several types of broadband dual-polarized antennas are proposed in references [1]–[15], including patch antennas, magnetoelectric dipole antennas and crossed dipole antennas. Patch antennas [1]–[3] have the advantages of compact size and low profile. However, they have several weaknesses, such as, high cross-polarization and large variations in gain and beamwidth over the operating band. Magnetoelectric dipole antennas are complicated in structure and large in size [4], [5], although they can achieve wide bandwidth, high isolation and stable radiation characteristics. Therefore, both the patch antennas and the magnetoelectric dipole antennas are not suitable for the applications with the demands of wide bandwidth, stable beamwidth and compact size.

Crossed dipole antennas [7]–[15] are widely used in wireless communication systems because of wide bandwidth, good radiation characteristics, compact size and ease of construction. These dipoles are fed by DF structures (with the conductors of the coaxial cables connected directly to two arms of dipoles) or CF structures (with the conductors of the coaxial cables connected to the coupling baluns of antennas).

Crossed dipole antennas in [9]–[12] using the DF structures, are large in radiation aperture or high in profile to realize impedance matching. Circular-shaped dipoles are employed to achieve wide bandwidth characteristic in [9] and [10], and the aperture is relatively larger compared with the square loop dipoles. Antennas reported in [11] and [12] both have wideband performance at the cost of high profile and large volume. It can be seen that the dipoles fed by DF structures are not easy to realize balanced impedance matching, because the conductors of the coaxial cables are connected directly to two arms of the dipoles. Since the coupling baluns can improve the impedance characteristics, the works in [13]–[15] using CF structures, are relatively compact in size and wide in bandwidth. However, the isolation deteriorates to around 27 dB as two resonant frequencies of crossed dipoles move apart to get wide bandwidth. Therefore, crossed dipole antennas with DF or CF structures cannot well meet the requirements of miniaturization applications, especially the indoor beamforming antenna array applications.

In this paper, a crossed dipole antenna using MDF structure is proposed to realize high isolation (33 dB) and compact size ($45 \times 45$ mm$^2$). Four pairs of square-shaped loop dipoles are utilized in the proposed antenna fed by coaxial cable directly. Compared with the conventional crossed dipole antennas with two pairs of dipoles, two additional pairs of dipoles are introduced to play the roles of coupling baluns and radiators at the same time. The symmetrical structure improves the isolation up to 33 dB. As a result, the proposed antenna using the MDF structure achieves good characters of both the DF and CF structures simultaneously, including balanced matching, high isolation, low cross-polarization and compact size. Besides, the gap structure of dipole arms adjacent to each other is designed in elliptical shape to improve the impedance characteristic. Therefore, the size of the antenna is further reduced to $45 \times 45$ mm$^2$ ($0.25\lambda_L \times 0.25\lambda_L$, where $\lambda_L$ is the free-space wavelength at 1.7 GHz, the lowest operating frequency) with VSWR $< 1.5$, due to the MDF structure and elliptical-shaped (ES) gap structure.

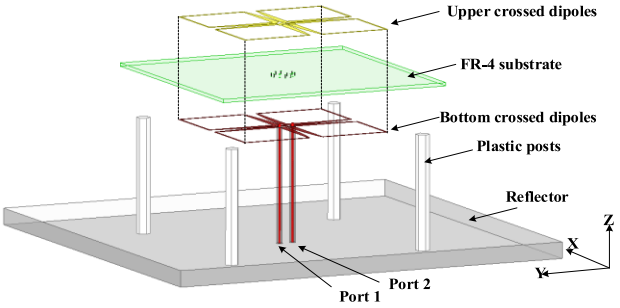


**FIGURE 1.** Structure of the proposed antenna.

## II. ANTENNA ELEMENT DESIGN

### A. STRUCTURE OF ANTENNA ELEMENT

The overall structure of the proposed antenna is shown in Fig. 1. It consists of one substrate printing four pairs of loop dipoles, two coaxial feeding cables, and a box-shaped reflector. For the substrate, there are two pairs of loop dipoles printed on top layer of the substrate, and two pairs of loop dipoles printed on bottom layer of the substrate. These four pairs of dipoles are fed by two coaxial cables. The substrate is supported by four plastic posts above the reflector.

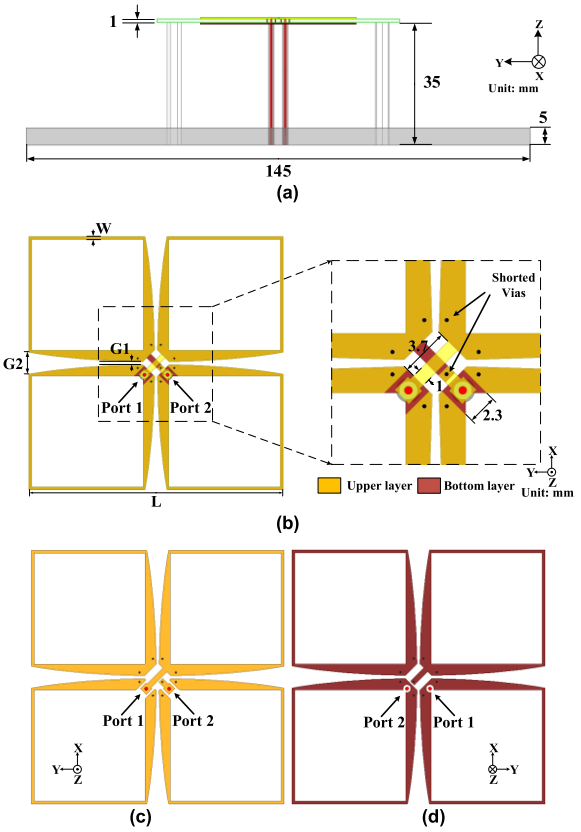


**FIGURE 2.** Detailed geometry of the proposed antenna. (a) Side view. (b) MDF structure. (c) Top view. (d) Bottom view. (Unit: mm. L = 45, W = 0.5, G1 = 0.5, G2 = 3.9).

The detailed structure of the antenna is shown in Fig. 2. All the loop dipoles are printed on a FR-4 substrate with a dielectric constant $\varepsilon_r = 4.4$, a loss tangent of 0.02, and a thickness of 1 mm, and the analyses are carried out by Ansys HFSS. Each layer of the substrate has two crossed dipoles printed with the same size and shape. Two pairs of loop dipoles are fed directly by coaxial cables, and the other two pairs of dipoles are connected to the two former pairs by eight shorted vias. The outer conductor of the coaxial cable is connected to one arm of the loop dipole on the bottom of the substrate. The inner conductor is extended through the substrate and connected to the other arm by a metallic strip. In order to avoid overlap, one of the metallic strips is modified by printing its partial line on the bottom layer of the substrate, and a metallic via is used to connect the upper and bottom parts of the feeding metallic strip. Beneath the substrate, a square box-shaped reflector is employed with a distance H = 35 mm (about $0.25\lambda_0$, where $\lambda_0$ is the free-space wavelength at 2.2 GHz) to realize a unidirectional radiation. The size of the reflector is $145 \times 145$ mm$^2$ and the height of wall

is 5 mm. Due to the symmetry of the structure of the antenna, there are the same performance for two ports. Therefore, all the analyses of the proposed antenna are implemented on port 1 in the following content.

### B. ANALYSIS OF ANTENNA ELEMENT

As is well known, the crossed dipole antenna is composed of two pairs of dipole antennas, which are placed orthogonally to each other to achieve dual polarization. According to [7] and [8], when one pair of dipoles is driven, the crossed one behaves as a parasitic element. As a result, the impedance bandwidth is widened intensively due to the utilization of strong coupling between the driven element and the parasitic element. However, the bandwidth of the loop dipoles is still not wide enough to cover 1.7-2.7 GHz. In order to improve the bandwidth and impedance matching, several different gap structures between the crossed dipoles are proposed in [8]–[10] and [15]. Stepped gap structures are applied in [8] and [15] to adjust two resonant modes, while wedge-shaped gaps are adopted in [9] and [10] to widen the impedance bandwidth. It can be seen that all these approaches are designed to add one more degree of freedom to control two resonant modes. These two resonant modes are moved apart by altering the gap structures to gain wider impedance bandwidth. In this paper, the gap structure in elliptical shape is proposed. The gap width increases gradually from the center to the edge of the antenna. Technically, the wedge-shaped and stepped gap structures are the special cases of the ES gap structure. The ES structure is modified from the wedge-shaped gap structure by changing the straight lines into curved lines, which adds one more degree of freedom to realize impedance matching. For the antenna with stepped structure, as the number of steps increases, the performance becomes closer to that of antenna with ES gap structure.

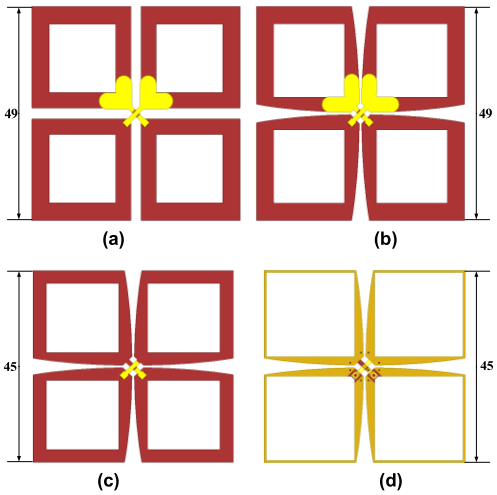


**FIGURE 3.** Structures of four types of antennas, (a) Type I: square loop dipoles, (b) Type II: CF structure, (c) Type III: DF structure, (d) Type IV: MDF structure (the proposed antenna). (Unit: mm).

Four types of antennas with the same height (H = 35 mm) are designed to demonstrate the evolution of the proposed antenna using the MDF structure, as shown in Fig. 3. Type I antenna consists of the square loop dipoles and CF structure. Compared with Type I, ES gap structure is adopted in Type II, without changing any other structures. Type II, III and IV has the same loop dipole structures with different parameter values, and are fed by CF, DF and MDF structures, respectively. Noting that the loop dipoles of Type I, II, III antennas are printed on the bottom layer of the substrate, while the loop dipoles of the proposed Type IV antenna are printed on both the top and bottom layer of the substrate. The sizes of Type I and II are both 49 × 49 mm$^2$, while the size of Type III and Type IV are 45 × 45 mm$^2$.

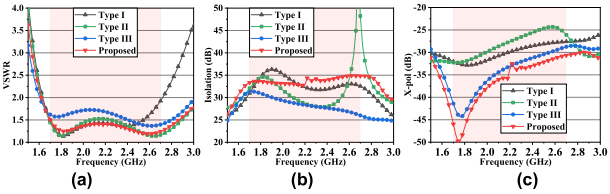


**FIGURE 4.** Simulated Results of four types of antennas. (a) VSWR. (b) Isolation. (c) Cross-polarization.

The simulated VSWR, isolation and cross-polarization of Type I, II, III, and IV (proposed antenna) are shown in Fig. 4. It can be seen that Type I is easy to realize unbalanced-to-balanced matching and high isolation (30 dB), but the impedance bandwidth is only 1.7-2.55 GHz which cannot occupy the range of 1.7-2.7 GHz. This simulated result validates the conclusion in [15]. Furthermore, the impedance bandwidth of Type II, III and IV with ES gap structures can be enhanced to 1.7-2.85 GHz (fractional bandwidth 51%). Compared with Type I, although the impedance bandwidth is broadened, the isolation of Type II deteriorates to around 27 dB as two resonant modes moves apart to get wide bandwidth [13]–[15]. The gap structure is adjusted to control the coupling between the crossed dipoles, and two resonant modes are moved apart to get wide bandwidth by increasing the gap width. However, as the gap becomes wider, the isolation between two ports would deteriorate. Likewise, the isolation of the proposed antenna is also influenced by the wider gap width, which will be analyzed in the following content. Fortunately, the proposed antenna maintains higher isolation because of the more symmetrical and compact structure. In order to miniaturize radiation aperture (45 × 45 mm$^2$), the DF structure is utilized in Type III with the bandwidth no change, and the VSWR worsens to more than 1.5 because of the unbalanced matching [11]. The antennas with DF structures are more compact, because they use the feeding structure as part of the radiator.

It is worth noting that, although the proposed antenna (Type IV) is fed directly by coaxial cables similarly to Type III antenna, two additional pairs of dipoles are employed as coupling baluns and radiators simultaneously. Firstly, these two additional pairs of dipoles play the roles as parts of radiator, just like another two pairs of dipoles. Secondly, by introducing capacitive coupling to the antenna, these two

additional pairs of dipoles make the antenna with DF structure able to realize unbalanced-to-balanced matching. As a consequence, the proposed antenna with more symmetrical structure has the advantages of both the DF and CF structures, such as, balanced matching, high isolation, low cross-polarization and compact size.

**TABLE 1. Comparison Of four type antennas.**

| Type | Bandwidth | Iso. (dB) | X-pol (dB) | Aperture (mm) |
|---|---|---|---|---|
| I: Square | × (1.7-2.55 GHz) | √ (31) | × (27) | × (49) |
| II: Coupling | √ (1.7-2.85 GHz) | × (27) | × (24) | × (49) |
| III: Direct | × (1.5<VSWR<2) | × (26) | √ (29) | √ (45) |
| IV: Proposed | √ (1.7-2.85 GHz) | √ (33) | √ (30) | √ (45) |

The comparison of bandwidth, isolation, cross-polarization and aperture among the four types of antennas is summarized in Table 1. It is clear that the proposed antenna (Type IV) has a wide bandwidth of 1.7-2.85 GHz, highest isolation of more than 33 dB, lowest cross-polarization of 30 dB and smallest aperture of 45 × 45 mm$^2$. The radiation patterns comparison between the propose antenna and Type II antenna in horizontal plane ($\varphi = 90°$) at 1.7, 2.2 and 2.7 GHz are shown in Fig. 5. It is clear that the cross-polarization and XPD of the proposed antenna are better than that of Type II antenna, especially in the higher band. Moreover, the co-polarization is more symmetrical at 2.7 GHz and more stable within the whole working frequencies.

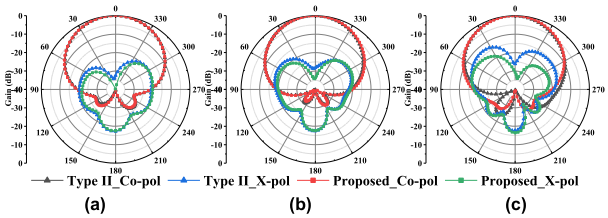


**FIGURE 5. Radiation patterns comparison between the proposed antenna and Type II antenna at the horizontal plane at (a) 1.7 GHz, (b) 2.2 GHz and (c) 2.7 GHz.**

Fig. 6(a), (b), (c) and (d) show the impacts of parameters L, W, G1 and G2, respectively, on VSWR and isolation. It can be seen from Fig. 6(a) that the lower resonant frequency moves downwards the lower frequency as L increases, while the isolation has almost no change. In the Fig. 6(b), the lower resonant frequency moves downwards the lower frequency as W decreases, while the isolation improves a little in higher frequency band. In order to achieve compact size, reasonable bandwidth and high isolation, L and W are set 45 mm and 0.5 mm, respectively. As shown in Fig. 6(c), the impedance matching of two resonant frequencies can be adjusted by G1. Here, G1 is set 0.5 mm to ensure two resonant frequencies match well at the same time to gain wide bandwidth. As plotted in Fig. 6(d), two resonant modes move apart and the bandwidth becomes wider when G2 increases, but the isolation and the impedance matching would deteriorate. For obtaining high isolation and wide bandwidth, G2 is set an

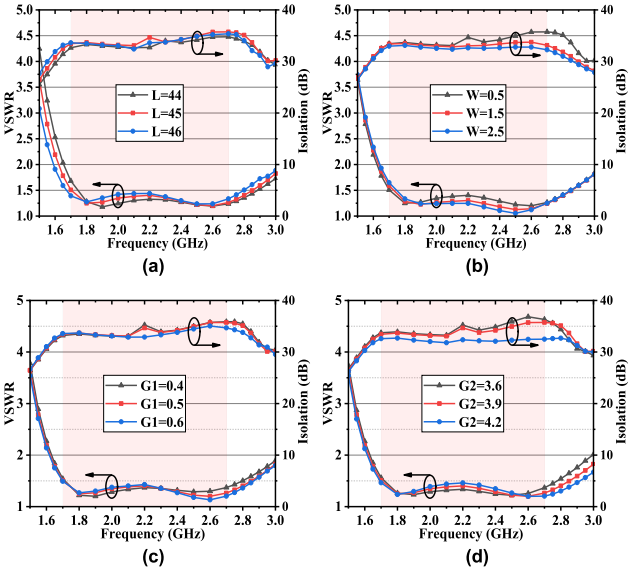


**FIGURE 6. Impacts of (a) L, (b) W, (c) G1 and (d) G2 on VSWR and isolation.**

optimized value 3.9 mm. Therefore, we can conclude that the lower resonant frequency is mainly controlled by L and W, the higher resonant frequency can be adjusted by G1 and G2, and the isolation is mainly influenced by G2.

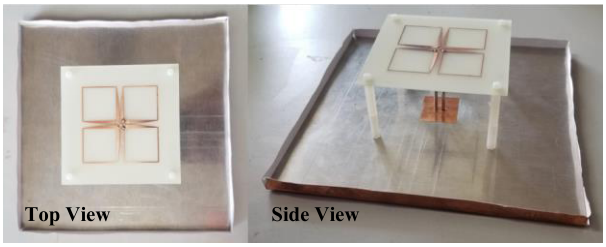


**FIGURE 7. The fabrication of the proposed antenna**

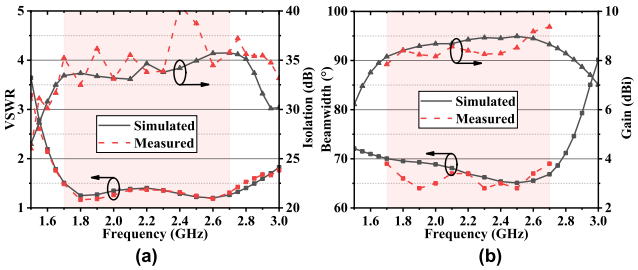


**FIGURE 8. Simulated and measured (a) VSWR and isolation and (b) HPBW and gain of the proposed antenna.**

### *C. PERFORMANCE OF ANTENNA ELEMENT*

The prototype and fabrication of the proposed antenna are depicted in Figs. 1 and 7, respectively. The measured results, including VSWR, isolation, gain, and radiation patterns, are obtained by an Agilent network analyzer (Agilent N5230A) and a far-field measurement system (NSI 2000). Fig. 8(a) shows the simulated and measured VSWR and isolation of the antenna element. Because the isolation is related with

the gap near the feeding structure, the deviation between the simulated and measured results could be attributed to SMA connector and fabrication tolerance. The overlapped impedance bandwidth of two ports is from 1.7 to 2.85 GHz with VSWR $< 1.5$, while the isolation is greater than 33 dB. The simulated and measured gain and HPBW at the horizontal ($\varphi = 90°$) plane versus frequency are depicted in Fig. 8(b). The measured gain is $8.5 \pm 0.6$ dBi from 1.7 to 2.7 GHz, which meets the simulated one, $8.6 \pm 0.4$ dBi. The measured HPBW is $66.5° \pm 2.5°$ at the horizontal plane, agreeing with the simulated result, $67.5° \pm 2.5°$. The simulated and measured radiation patterns at the horizontal plane at different frequencies of 1.7, 2.2, and 2.7 GHz are plotted in Fig. 9, which shows that the antenna has stable radiation patterns with low cross-polarization (30 dB) across the entire bands of 2G/3G/4G. The measured radiation patterns agree well with the simulated ones. It is worth mentioning that the proposed antenna achieves more stable cross-polarization discrimination (XPD) than CF crossed dipoles within $\pm 60°$.

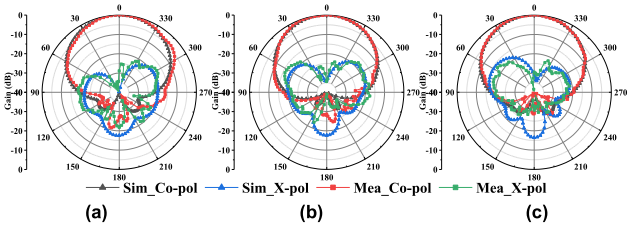


**FIGURE 9.** Simulated and measured radiation patterns at the horizontal plane at (a) 1.7 GHz, (b) 2.2 GHz and (c) 2.7 GHz.

**TABLE 2.** Comparison Of different feeding structures.

| Ref. | | Bandwidth | Radiation Aperture ($mm^2$) | H (mm) | Iso. (dB) | X-pol (dB) |
|---|---|---|---|---|---|---|
| Direct feeding structure | 9 | 1.7-2.7 (RL>15) | 55×55 | 36 | 30 | 20 |
| | 10 | 1.68-2.77 (VSWR<1.4) | 59×59 | 36 | 28 | NM |
| | 11 | 1.45-2.75 (RL>10) | 48×48 | 45 | 40 | 26 |
| | 12 | 1.61-2.71 (RL>15) | 70×70 | 42 | 30 | 28 |
| Coupling feeding structure | 13 | 1.7-2.7 (SWR<1.5) | 53×53 | 34 | 25 | NM |
| | 14 | 1.68-2.83 (RL>15) | 52.4×52.4 | 35 | 27 | 27 |
| | 15 | 1.68-2.94 (VSWR<1.5) | 50.5×50.5 | 35 | 28.5 | 25 |
| This work (MDF) | | 1.7-2.8 (VSWR<1.5) | 45×45 | 35 | 33 | 30 |

Table 2 presents a comparison of some reported antennas [9]–[15] and the proposed antenna. All the reference antennas are printed on substrates and excited with the DF structures or the CF structures. The antennas in [9]–[12] using the DF structures, realize wideband unbalanced-to-balanced matching at the price of large radiation aperture or high profile. The works in [13]–[15] using the CF structures, have compact size and wide bandwidth while their isolations are not good enough (around 27 dB). It can be seen clearly that the proposed antenna using the MDF structure has the advantages of the smallest aperture size and relatively high isolation and low cross-polarization.

## III. ANTENNA ARRAY

In order to investigate the performance of adjacent elements in the beamforming antenna array, a two-element array is designed as a demonstration.

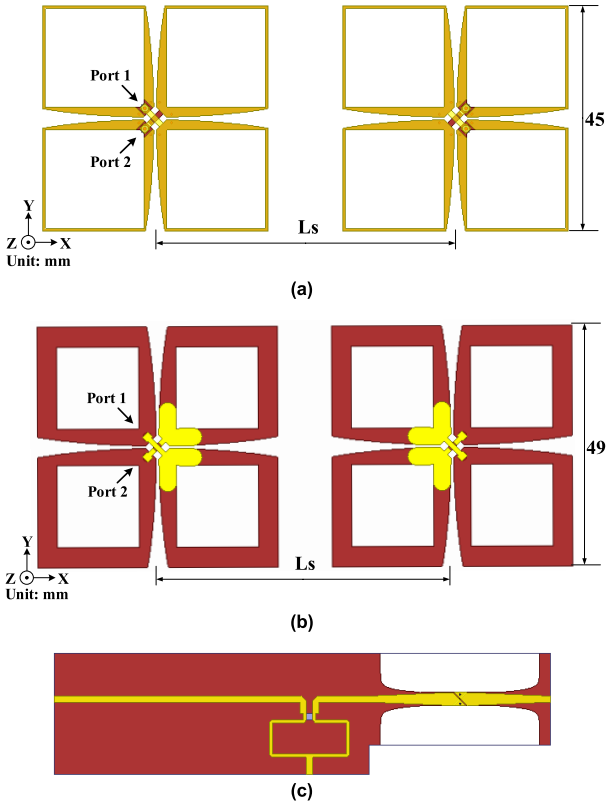


**FIGURE 10.** Configuration of the two-element array. (a) The proposed array. (b) The Type II array. (c) Configuration of the divider network.

### A. DESIGN OF ANTENNA ARRAY

The proposed two-element antenna array is shown in Fig. 10(a). It consists of two antenna elements designed in the Section II. These two antenna elements are fed by an out-of-phase power divider, shown in Fig. 10(c), and are placed away from each other with the distance of Ls. As reference, the Type II antenna array composed of two type II antenna elements, is shown in Fig. 10(b). In order to achieve more stable and symmetrical radiation patterns and suppress the cross-polarization of the array, the feeding portions of these two elements are located at opposite directions [1].

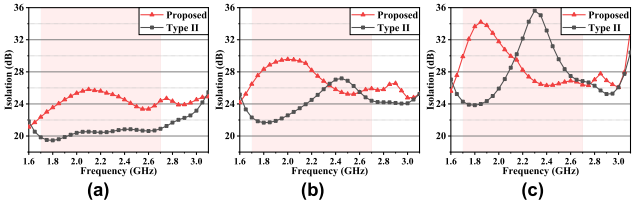


**FIGURE 11.** Simulated isolation of the Type II array and the proposed array in the distance of (a) Ls = 80mm, (b) Ls = 100mm and (c) Ls = 120mm.

Fig. 11 shows the simulated isolation of the Type II array and the proposed array in different distances. In the distance of Ls = 80, 100 and 120 mm, the isolations of the proposed array are higher than 22, 25 and 26 dB, while the isolations

of the Type II array are higher than 19, 22 and 24 dB. It can be observed that the proposed array achieves higher isolation than the Type II array, especially in the lower frequency band.

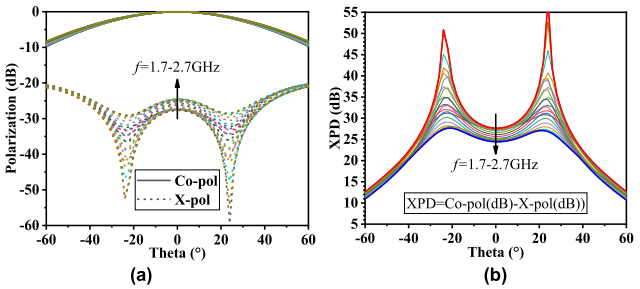


**FIGURE 12.** The (a) CP and XP and (b) XPD = CP(dB) - XP(dB) of the proposed array from 1.7-2.7 GHz.

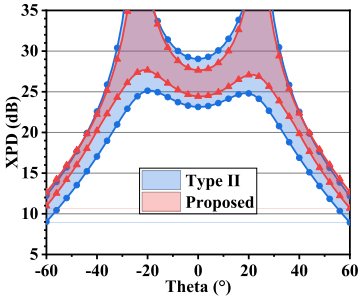


**FIGURE 13.** The XPD of the Type II array and the proposed array with the distance Ls = 100 mm.

The co-polarization (CP) and cross-polarization (XP) are plotted in Fig. 12(a), and the CP is stable while the XP become a little worse with the frequency increasing. The cross-polarization discrimination (XPD) [17] is plotted in Fig. 12(b), and the XPD changes with the frequency increasing. Fig. 13 shows the simulated XPD of the Type II array and the proposed array with the distance Ls = 100 mm. The XPD of the proposed array are higher than 10.5 dB, and the XPD of the Type II array are higher than 8.8 dB. Compared with the Type II array, the proposed array has higher XPD, which is more than 10.5 dB within ± 60° of the main lobe at the horizontal plane.


**FIGURE 14.** The fabrication of the proposed two-element antenna array.

### *B. PARAMETERS OF ANTENNA ARRAY*

The prototype and fabrication of the proposed two-element array are depicted in Figs. 10(a) and 14, respectively.

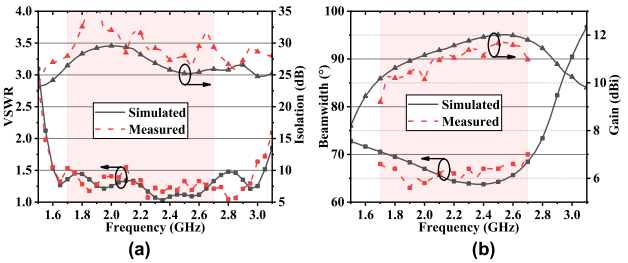


**FIGURE 15.** Simulated and measured (a) VSWR and isolation and (b) HPBW and gain of the proposed array.

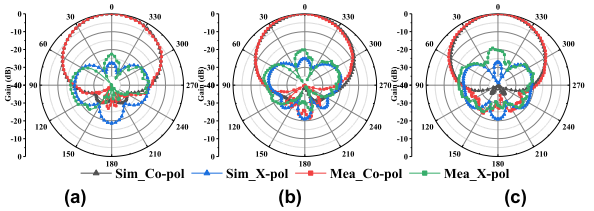


**FIGURE 16.** Simulated and measured radiation patterns at the horizontal plane at (a) 1.7 GHz, (b) 2.2 GHz and (c) 2.7 GHz.

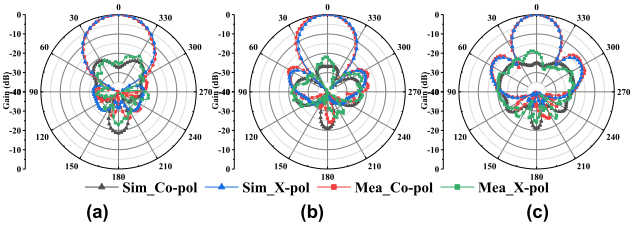


**FIGURE 17.** Simulated and measured radiation patterns at the vertical plane at (a) 1.7 GHz, (b) 2.2 GHz and (c) 2.7 GHz.

For verification, the distance Ls = 100 is selected. Fig. 15(a) shows the simulated and measured VSWR and isolation of the two-element antenna array with the out-of-phase power divider matching network. The total bandwidth is broadened to 1.6-2.95 GHz (59.3%), and the isolation (25 dB) is still at a relatively high level under the condition of Ls = 100 mm ($0.53\lambda_L$, $\lambda_L$ is the free-space wavelength at 1.6 GHz). The simulated and measured gain and HPBW at the horizontal plane versus frequency are depicted in Fig. 15(b). The measured gain is 10.5 ± 1.3 dBi from 1.7 to 2.7 GHz. It is around 0.5 dB lower than the simulated gain, mainly because of the insertion losses cost by the power divider network and coaxial cable. The measured HPBW is 66.5° ± 3.5° at the horizontal plane ($\varphi = 90°$), agreeing well with the simulated result. The simulated and measured radiation patterns at the horizontal plane at 1.7, 2.2, and 2.7 GHz are plotted in Fig. 16. It can be seen that the measured XPD is more than 20 dB at the boresight and more than 10 dB within ± 60°. The simulated and measured radiation patterns at the vertical plane at 1.7, 2.2, and 2.7 GHz are plotted in Fig. 17. As shown in Fig. 17, since the array spacing is small, the radiation patterns at the vertical plane has low sidelobes. The small spacing and low

sidelobes could make contribution to indoor beamforming of antenna array.

## IV. CONCLUSION

A compact wideband dual-polarized antenna with high isolation using MDF structure is proposed in this paper. The antenna achieves a wide impedance bandwidth of 1.7-2.85 GHz for VSWR $< 1.5$ with the miniaturized size of $45 \times 45$ mm$^2$ and high isolation of more than 33 dB. A two-element array with a small distance Ls $= 100$ mm configured by out-of-phase power divider is developed. High isolation of 25 dB and broadened bandwidth of 1.6-2.95 GHz (59.3%) are obtained. Therefore, the proposed antenna could be a good candidate for base station applications, especially the indoor beamforming antenna array applications.

## REFERENCES

[1] T. P. Wong and K. M. Luk, "A wide bandwidth and wide beamwidth CDMA/GSM base station antenna array with low backlobe radiation," *IEEE Trans. Veh. Technol.*, vol. 54, no. 3, pp. 903–909, May 2005.

[2] J. Zhang, X. Q. Lin, L. Y. Nie, J. W. Yu, and Y. Fan, "Wideband dual-polarization patch antenna array with parallel strip line balun feeding," *IEEE Antennas Wireless Propag. Lett.*, vol. 15, pp. 1499–1501, 2016.

[3] F. Zhu *et al.*, "Ultra-wideband dual-polarized patch antenna with four capacitively coupled feeds," *IEEE Trans. Antennas Propag.*, vol. 62, no. 5, pp. 2440–2449, May 2014.

[4] K.-M. Luk and B. Wu, "The magnetoelectric dipole—A wideband antenna for base stations in mobile communications," *Proc. IEEE*, vol. 100, no. 7, pp. 2297–2307, Apr. 2012.

[5] Z. N. Chen and K. M. Luk, *Antennas for Base Stations in Wireless Communications*. New York, NY, USA: McGraw-Hill, 2009.

[6] M.-C. Tang, T. Shi, and R. W. Ziolkowski, "Electrically small, broadside radiating Huygens source antenna augmented with internal non-Foster elements to increase its bandwidth," *IEEE Antennas Wireless Propag. Lett.*, vol. 16, pp. 712–715, 2017.

[7] Z. Bao, Z. Nie, and X. Zong, "A novel broadband dual-polarization antenna utilizing strong mutual coupling," *IEEE Trans. Antennas Propag.*, vol. 62, no. 1, pp. 450–454, Jan. 2014.

[8] D.-Z. Zheng and Q.-X. Chu, "The design of dual-polarized antenna for base station applications," in *Proc. 10th Eur. Conf. Antennas Propag. (EuCAP)*, Davos, Switzerland, Apr. 2016, pp. 1–4.

[9] Y. Cui, R. Li, and H. Fu, "A broadband dual-polarized planar antenna for 2G/3G/LTE base stations," *IEEE Trans. Antennas Propag.*, vol. 62, no. 9, pp. 4836–4840, Sep. 2014.

[10] H.-J. Xu, X.-W. Zhu, and Z.-Q. Kuai, "Broadband dual-polarized planar antenna and array for mobile communication base station," in *Proc. Asia–Pacific Microw. Conf. (APMC)*, Nanjing, China, Feb. 2015, pp. 1–3.

[11] F. Alizadeh, C. Ghobadi, J. Nourinia, and B. Mohammadi, "A compact and wideband slotted dual-polarized antenna with high-isolation and low cross-polarization," in *Proc. Iranian Conf. Elect. Eng. (ICEE)*, Tehran, Iran, Jul. 2017, pp. 1874–1877.

[12] Y. Cui and R. Li, "Analysis and design of a broadband dual-polarized planar antenna for 2G/3G/4G base stations," in *Proc. 11th Eur. Conf. Antennas Propag. (EUCAP)*, Paris, France, May 2017, pp. 2143–2147.

[13] Q.-X. Chu, D.-L. Wen, and Y. Luo, "A broadband ±45° dual-polarized antenna with Y-shaped feeding lines," *IEEE Trans. Antennas Propag.*, vol. 63, no. 2, pp. 483–490, Feb. 2015.

[14] D.-Z. Zheng and Q.-X. Chu, "A multimode wideband ±45° dual-polarized antenna with embedded loops," *IEEE Antennas Wireless Propag. Lett.*, vol. 16, pp. 633–636, Jul. 2017.

[15] D.-Z. Zheng and Q.-X. Chu, "A wideband dual-polarized antenna with two independently controllable resonant modes and its array for base-station applications," *IEEE Antennas Wireless Propag. Lett.*, vol. 16, pp. 2014–2017, 2017.

[16] K. Hagiwara and H. Arai, "Wideband unbalanced fed 180-degree phase shifter using phase inverter," in *Proc. IEEE Int. Workshop Electromagn., Appl. Student Innov. Competition*, Kowloon, China, Sep. 2013, pp. 76–77.

[17] Y. Luo, Q.-X. Chu, and D.-L. Wen, "A plus/minus 45 degree dual-polarized base-station antenna with enhanced cross-polarization discrimination via addition of four parasitic elements placed in a square contour," *IEEE Trans. Antennas Propag.*, vol. 64, no. 4, pp. 1514–1519, Apr. 2016.

**YAOHUI ZHANG** received the B.S. degree in electromagnetic wave propagation and antenna from the University of Electronic Science and Technology of China, Chengdu, China, in 2014, where he is currently pursuing the Ph.D. degree in electromagnetic field and microwave technology.

His research interests include compact and wideband antennas and microwave filter.

**DAOTONG LI** (S'15–M'16) received the Ph.D. degree in electromagnetic field and microwave technology from the University of Electronic Science and Technology of China (UESTC), Chengdu, China, in 2016.

He is currently with the Center of Aircraft TT&C and Communication, Chongqing University, Chongqing. Since 2015, he has been a Visiting Researcher with the Department of Electrical and Computer Engineering, University of Illinois at Urbana–Champaign, Urbana, IL, USA, with the financial support from the China Scholarship Council. He has authored or co-authored over 30 peer-reviewed journal or conference papers. Since 2014, he has been a reviewer for some international journals.

His current research interests include RF, microwave and millimeter-wave technology and applications, antennas, devices, circuits and systems, and passive and active (sub-) millimeter-wave imaging and radiometer. He was a recipient of the UESTC Outstanding Graduate Awards by the Sichuan Province and UESTC in 2016, the National Graduate Student Scholarship from the Ministry of Education, China, and the "Tang Lixin" Scholarship.

**YONGHONG ZHANG** received the B.S., M.S., and Ph.D. degrees from the University of Electronic Science and Technology of China (UESTC), Chengdu, China, in 1992, 1995, and 2001, respectively.

He is currently a Full Professor with the School of Electronic Science and Engineering, UESTC. From 1995 to 2002, he was a Lecturer at UESTC. From 2002 to 2004, he was a Post-Doctoral Fellow at the Department of Electronic Engineering, Tsinghua University, Beijing, China. Since 2004, he has been with UESTC. His research interests are in the area of microwave and millimeter wave technology and applications. He is a Senior Member of the Chinese Institute of Electronics.

**YONG FAN** (M'05) received the B.E. degree from the Nanjing University of Science and Technology, Jiangsu, China, in 1985, and the M.S. degree from the University of Electronic Science and Technology of China, Chengdu, China, in 1992.

He is currently a Full Professor with the School of Electronic Science and Engineering, University of Electronic Science and Technology of China. He has authored or co-authored over 200 papers. His current research interests include electromagnetic theory, millimeter-wave and Terahertz Circuits, and communication technology. He is a Senior Member of the Chinese Institute of Electronics.